ChemPubSoc Europe

DOI: 10.1002/chem.201600066

CHEMISTRY A European Journal Communication

Porphyrinoids

Chemo- and Regioselective Reduction of 5,15-Diazaporphyrins Providing Antiaromatic Azaporphyrinoids

Ayaka Yamaji,[a] Hayato Tsurugi,[b] Yoshihiro Miyake,*[a] Kazushi Mashima,[b] and Hiroshi Shinokubo*[a]

Abstract: Reagent-controlled chemo- and regioselective reduction of 5,15-diazaporphyrins has been developed. The selective reduction of carbon–carbon double bonds of diazaporphyrins provides 18π aromatic isobacteriochlorin-type products, whereas the reduction of carbon–nitrogen double bonds leads to selective formation of 20π *N*,*N*′-dihydrodiazaporphyrins in excellent yields. The distinct antiaromatic character of *N*,*N*′-dihydrodiazaporphyrins has been revealed. The free-base *N*,*N*′-dihydrodiazaporphyrin exhibits slower inner NH tautomerism than that in the corresponding 18π porphyrins.

Porphyrinoids have attracted considerable attention, owing to their excellent optical and electronic properties. Redox processes of porphyrinoids are a promising route for the creation of novel and unique π-conjugated skeletons, because these processes can change the structures and the number of π electrons in the conjugated circuits. Reduction of regular porphyrins at the peripheral double bonds of the pyrrole units provides aromatic chlorins, bacteriochlorins, and isobacteriochlorins, which are the key structures of chlorophylls (Figure 1).[1] Reduction of carbon–carbon double bonds at the *meso* positions of porphyrins leads to phlorins, which show nonaromatic behavior.[2] However, isophlorins, obtained from reduction of two imine moieties of porphyrins, are known to have nonplanar 20π-electron systems.[3] In general, free-base isophlorins adopt highly distorted conformations due to the steric repulsion among the four NH protons in the central cavity. Chen and co-workers reported a 20π free-base isophlorin that shows a nonaromatic nature because of the nonplanar saddle conformation.[4] In 2005, Vaid and co-workers reported the synthesis of an antiaromatic 20π silicon(IV) porphyrin with a highly ruffled structure.[5] Since the isophlorin macrocycle works as a tetravalent ligand, the choice of central metals is limited.[6] The synthesis of 20π porphyrinoids with both high planarity and distinct antiaromaticity is still challenging.[7]

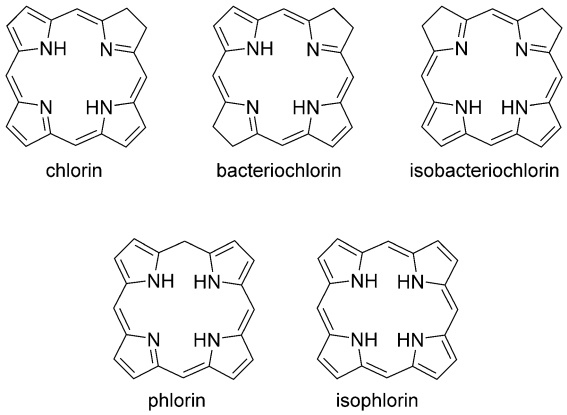

Figure 1. Reduction products of porphyrin.

5,15-Diazaporphyrins (**1 M**, Scheme 1; M = Ni or 2H) are 18π porphyrinoids with imine-type sp^2-hybridized nitrogen atoms at the *meso* positions.[8,9] Because of its relatively low-lying LUMO, **1 M** is prone to undergo nucleophilic addition of alkyllithium reagents.[8b] This characteristic feature of **1 M** prompted us to explore the reaction of **1 M** with various reductants.

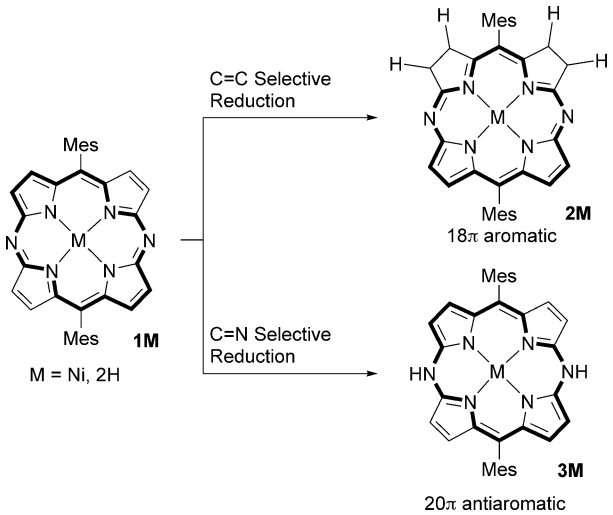

Scheme 1. Chemo- and regioselective reduction of 5,15-diazaporphyrins. Mes = 2,4,6-trimethylphenyl.

[a] *A. Yamaji, Prof. Dr. Y. Miyake, Prof. Dr. H. Shinokubo*
Department of Applied Chemistry, Graduate School of Engineering
Nagoya University, Nagoya 464-8603 (Japan)
E-mail: miyake@apchem.nagoya-u.ac.jp
hshino@apchem.nagoya-u.ac.jp

[b] *Prof. Dr. H. Tsurugi, Prof. Dr. K. Mashima*
Department of Chemistry, Graduate School of Engineering Science
Osaka University, Osaka 560-8531 (Japan)

Supporting information for this article is available on the WWW under http://dx.doi.org/10.1002/chem.201600066.

We have now succeeded in the development of reagent-controlled chemo- and regioselective reduction of 5,15-diazaporphyrins **1M** (Scheme 1). In this process, the selective reduction of carbon–carbon double bonds provided the 18π aromatic isobacteriochlorin-type product **2M**, whereas the reduction of carbon–nitrogen double bonds yielded *N*,*N*′-dihydrodiazaporphyrins **3M** selectively. The planar structure and 20π conjugation, including lone pairs on the nitrogen atoms at the *meso* positions, induce distinct antiaromatic character of **3M**. In contrast to isophlorins, free-base *N*,*N*′-dihydrodiazaporphyrin **3H$_2$** has two NH protons in the central cavity, which is similar to normal porphyrins.

We conducted the reaction of **1Ni** with a hydride reagent (Scheme 2). Treatment of **1Ni** with 12 equivalents of $NaBH_4$ in the presence of Pd/C[10] in CH_2Cl_2/MeOH (3:1) at room temperature for 2 h afforded **2Ni** as a single isomer in 79% yield with a trace amount of chlorine-type product **4Ni**. In the absence

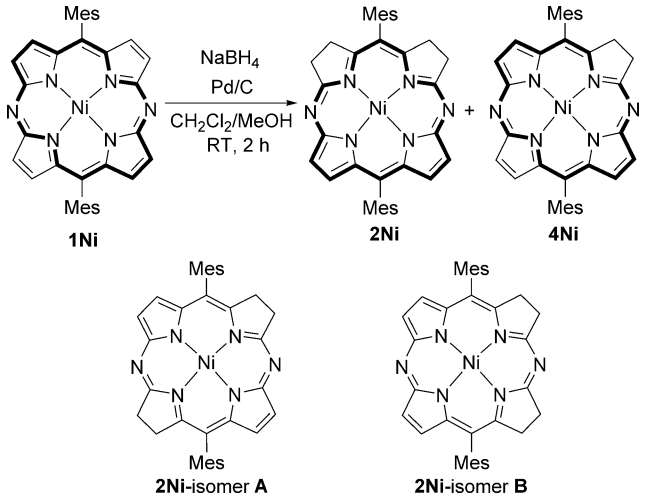

Scheme 2. Reduction of **1Ni** with $NaBH_4$.

of Pd/C, **2Ni** and **4Ni** were obtained in 13% and 14% yields, respectively. The X-ray diffraction analysis of **2Ni** revealed the high planarity of the macrocycle of **2Ni**. Unfortunately, the assignment of **2Ni** was not conclusive because three regioisomers **2Ni**, **2Ni**-isomer **A**, and **2Ni**-isomer **B** could not be distinguished by the X-ray analysis because of the highly disordered structure (see the Supporting Information, Figure S11).[11] The ^{1}H NMR spectrum of **2Ni** displayed two doublet peaks for β-protons in the aromatic region at $\delta = 7.5$ ppm and protons on sp^3 carbons at $\delta \approx 3.0$–4.0 ppm, suggesting C_{2v} symmetry. The ^{13}C NMR spectrum of **2Ni** also indicated that the structure of **2Ni** adopted C_{2v} symmetry. On the basis of these NMR data, we concluded that **2Ni** has the isobacteriochlorin-type structure with 18π aromatic conjugation.

A proposed reaction pathway for the reduction of **1Ni** to **2Ni** is shown in Scheme 3. In this reduction process, the attack of hydride at the pyrrole rings should be a key step for the selective reduction of carbon–carbon double bonds. The initial nucleophilic attack of hydride would occur at the C3 position because of a directing effect of the outer nitrogen atom

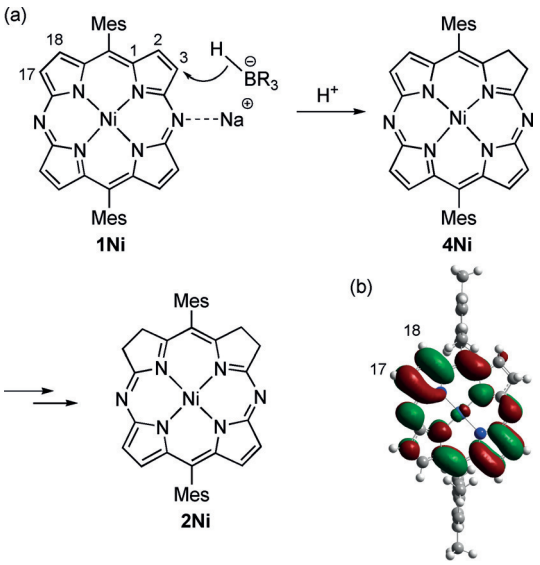

Scheme 3. a) Proposed reaction pathway for the reduction of **1Ni** to **2Ni**; b) DFT-calculated molecular orbitals of **4Ni**.

through coordination with the sodium cation.[8b] Protonation of the initial adduct then affords **4Ni**. The DFT calculation of **4Ni** at the B3LYP/6-31G(d) + SDD level suggests that the MO coefficient at the C17 position in the LUMO of **4Ni** is significantly larger than those at other β-positions (Scheme 3b). Consequently, formation of **2Ni** should be favored in reduction with $NaBH_4$ over the bacteriochlorin-type reduction product.

Figure 2 shows the electronic absorption spectra of **1Ni**, **2Ni**, and **4Ni** in CH_2Cl_2. The characteristic changes of the absorption features of these compounds are consistent with the general trend that is typically observed from porphyrin to chlorine and isobacteriochlorin.[1] The Q-band of chlorin-type

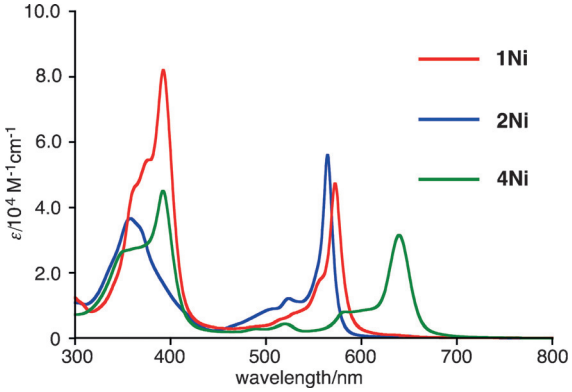

Figure 2. Electronic absorption spectra of **1Ni**, **2Ni**, and **4Ni** in CH_2Cl_2.

4Ni was substantially redshifted. In comparison to **1Ni**, the Q-band of **2Ni** was hypsochromically shifted. This shift is well supported by the DFT calculations. The calculated HOMO–LUMO gaps of **1Ni**, **2Ni**, and **4Ni** were 2.73, 2.83, and 2.45 eV, respectively. The relative intensity of the Q-band to the Soret

band increased in the order of **1 Ni**, **4 Ni**, and **2 Ni**, as the number of reduced double bonds increased.

We then found that the use of *N*,*N*′-bis(trimethylsilyl)-1,4-dihydropyrazine **5**[12] as a reductant for **1 M** cleanly and selectively furnished *N*,*N*′-dihydrodiazaporphyrins **3 M** (Scheme 4). *N*,*N*′-Disilyl-1,4-dihydropyrazine **5** serves as a versatile and strong reducing reagent for group 4–6 metal and late transition metal chlorides.[12b,c] When we carried out the reaction of **1 Ni** with 1.6 equivalents of **5** in THF at room temperature, complete conversion of **1 Ni** was confirmed by ^{1}H NMR spectroscopy. Treatment of the resulting solution with an excess amount of MeOH afforded **3 Ni** in 84% yield. This protocol was also applied to the reduction of free-base diazaporphyrin **1 H_2** and dihydrodiazaporphyrin **3 H_2** was obtained in 78% yield. Both **3 Ni** and **3 H_2** were easily oxidized back to diazaporphyrins **1 Ni** and **1 H_2**, respectively, in solution under air.

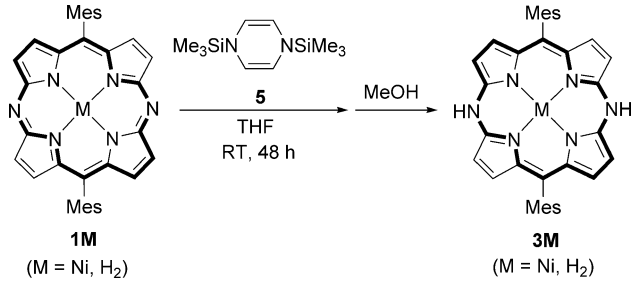

Scheme 4. Reduction of **1 M** with **5**.

The structures of **3 Ni**[13] and **3 H_2**[14] were unambiguously revealed by X-ray diffraction analysis (Figure 3). The skeletons of **3 Ni** and **3 H_2** are almost perfectly planar (Figure 3 b,d) with small mean plane deviations of 0.049 Å (**3 Ni**) and 0.031 Å (**3 H_2**). In addition, **3 Ni** and **3 H_2** display significant bond-length alternations, which are diagnostic for antiaromatic porphyrinoids (Figure 3 e). These results strongly suggest that **3 Ni** and **3 H_2** exhibit antiaromaticity, owing to planar 20π conjugation. The nucleus-independent chemical shift (NICS) values (calculated at points "**a**" and "**b**" in Figure 3 a,c) are +15.5 and +15.8 ppm, respectively, confirming the substantial paratropic ring current effect of **3 Ni** and **3 H_2**. Whereas 18π diazaporphyrin **1 Ni** exhibited β-protons in the aromatic region of $\delta = 8.8$–9.2 ppm in its ^{1}H NMR spectrum, the β-proton signals of **3 Ni** were shifted significantly upfield to $\delta = 3.0$–4.0 ppm. In addition, the inner two NH protons of **3 H_2** were observed in the downfield region at $\delta = 24.5$ ppm. These characteristic proton chemical shifts confirm the distinct antiaromatic natures of **3 Ni** and **3 H_2**. Free-base porphyrinoids with 4*n*π conjugation often adopt nonplanar conformations to relieve antiaromatic destabilization. The highly planar structure of **3 H_2** is probably maintained by the effective hydrogen bonding interactions in the central cavity,[15] as indicated by the highly downfield-shifted NH proton signals.

Unexpectedly, the ^{1}H NMR spectrum of **3 H_2** displayed no β-protons signals at room temperature. We then found that the spectrum of **3 H_2** was highly dependent on temperature

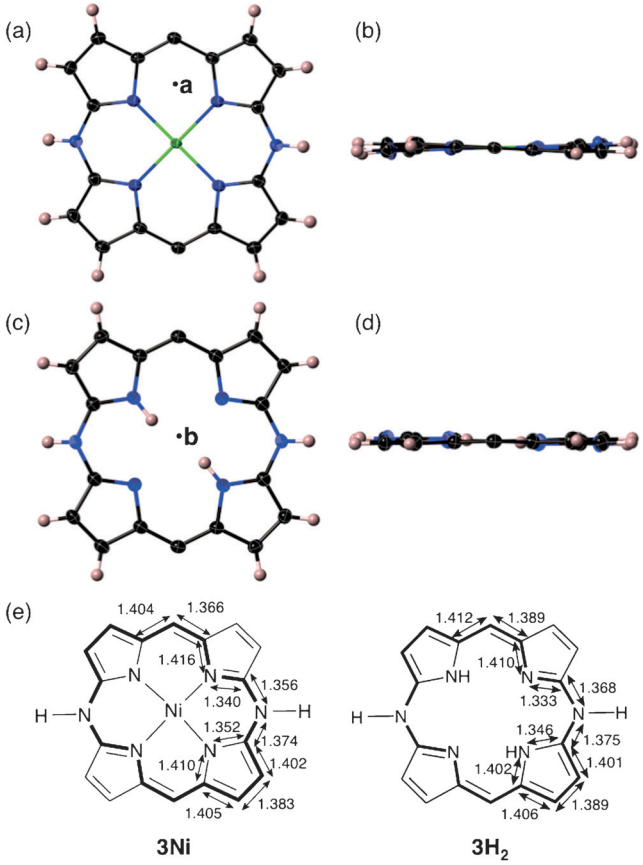

Figure 3. X-ray crystal structures of dihydrodiazaporphyrins. Thermal ellipsoids are scaled at 50% probability level. Mesityl groups are omitted for clarity: a) Top and b) side views of **3 Ni**; c) top and d) side views of **3 H_2**; e) bond length alternations of **3 Ni** and **3 H_2**.

(Figure 4). At −50 °C, four doublet signals for β-protons were detected at $\delta = 3.0$–4.5 ppm. As the temperature was raised, the four doublet signals were broadened, reaching a coalescence point at 25 °C, where the β-proton signals nearly disap-

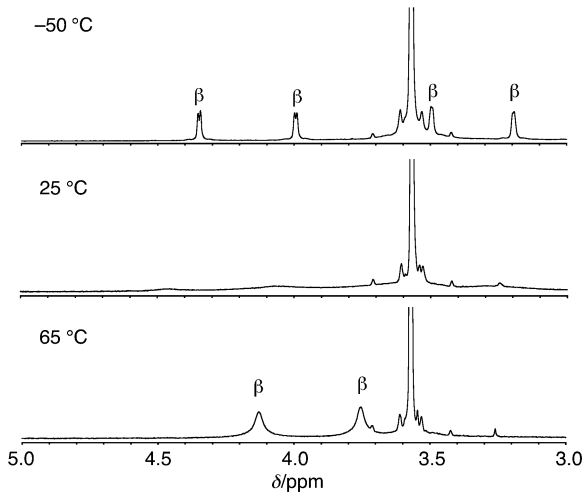

Figure 4. Variable-temperature NMR spectra of **3 H_2** at −50, 25, and 65 °C in [D_8]THF.

peared. Two broad signals then appeared at higher temperatures. We presumed that the spectral change with temperature resulted from the inner proton exchange of **3H$_2$**, in analogy to NH tautomerization of porphyrins (Scheme 5a).[16] The activation energy of inner proton exchange of **3H$_2$** was measured to be 14.3 kcal mol^{-1} at 25 °C.[17] This value is substantially larger than that of the energy barrier of NH proton exchange in typical porphyrins (ca. 12 kcal mol^{-1}).[16c]

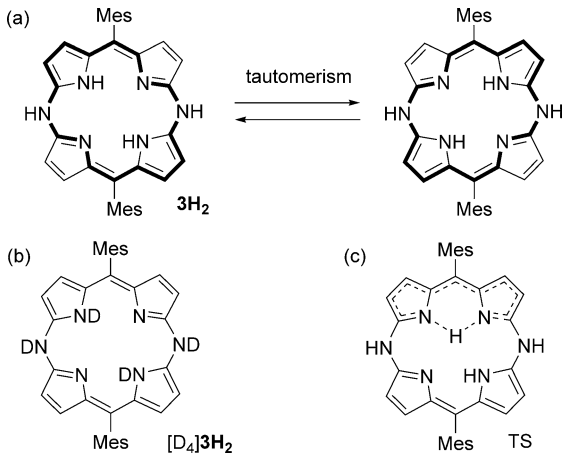

Scheme 5. a) Inner proton exchange in **3H$_2$**; b) [D$_4$]**3H$_2$**; c) transition state in tautomerization.

We then performed DFT calculations to obtain the transition-state structure for the inner NH migration reaction (Figure 5). Calculations were conducted at the B3LYP/6-31+G(d) level on model compounds in which the mesityl substituents were replaced with hydrogen atoms. The transition-state structure was obtained by the QST2 method. The activation energy was calculated to be 14.6 kcal mol^{-1}, which is in good agreement with the experimental value (14.3 kcal mol^{-1}).

Further evidence for our hypothesis was obtained by using the deuterium-labeled compound [D$_4$]**3H$_2$**. The coalescence temperature of [D$_4$]**3H$_2$** was 45 °C (see the Supporting Information, Figure S10). The activation barrier of [D$_4$]**3H$_2$** (15.3 kcal mol^{-1} at 45 °C) was higher than that of **3H$_2$** due to the kinetic isotope effect (Scheme 5b). As shown in the X-ray structure, dihydrodiazaporphyrin **3H$_2$** has rather localized π-bonds. This considerable bond length alternation of **3H$_2$** should be due to Jahn–Teller distortion.[18] However, the conjugation circuit is switched by NH tautomerism and π-bonds in the transition state (TS) should be delocalized (Scheme 5c). The temporal delocalization of π-electrons in the TS would enhance antiaromaticity to destabilize the TS, resulting in the larger activation barrier of NH tautomerization. In fact, the NICS value at the ring center of the TS is +21.0 ppm, which is substantially larger than that of **3H$_2$** (+16.1 ppm; Figure 5).

To elucidate the reaction pathway, we monitored the reaction of **1Ni** with **5** in [D$_8$]THF at room temperature by ^{1}H NMR spectroscopy (Scheme 6 and Figure S6 in the Supporting Information). After 1 h, **3Ni**, **3Ni-TMS**, and **3Ni-TMS$_2$** had formed in 38, 11, and 14% yields, respectively, alongside the recovery of 34% of **1Ni**. In addition, we also detected the formation of pyrazine. This result clearly shows that both the electron transfer from **5** to **1Ni** and the migration of trimethylsilyl (TMS) groups are key steps in the formation of **3Ni**.[12b] The initial step would be an electronic interaction between electron-deficient **1Ni** and electron-rich **5**, to provide the corresponding radical ion pair. Then, the cleavage of N–Si bonds in **5** and the formation of N–Si bonds in **3Ni-TMS$_2$** would furnish **3Ni-TMS$_2$** and pyrazine. Finally, **3Ni-TMS$_2$** is converted into **3Ni** through desilylation with methanol.

The UV/Vis absorption spectra of **3Ni** and **3H$_2$** are shown in Figure 6. The absorption spectra of **3Ni** and **3H$_2$** exhibit a substantially different shape from those of **1Ni** and **1H$_2$**.[8] In particular, weak absorption bands were detected at $\lambda = 700$–1200 nm (dashed lines) and are assigned to the characteristic forbidden bands that are typical for antiaromatic porphyrinoids.[19] The electrochemical properties of **3Ni** and **3H$_2$** were examined by using cyclic voltammetry (see the Supporting Information, Figure S13). The cyclic voltammograms of **3Ni** and

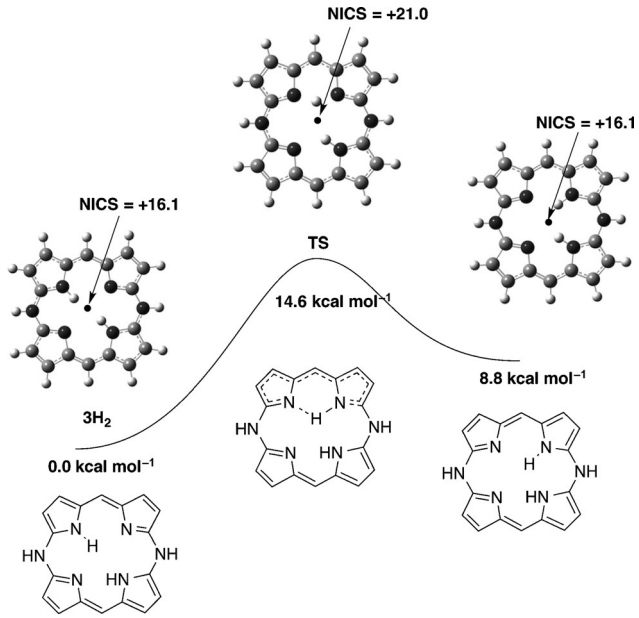

Figure 5. Calculated pathway of the inner proton exchange of **3H$_2$**.

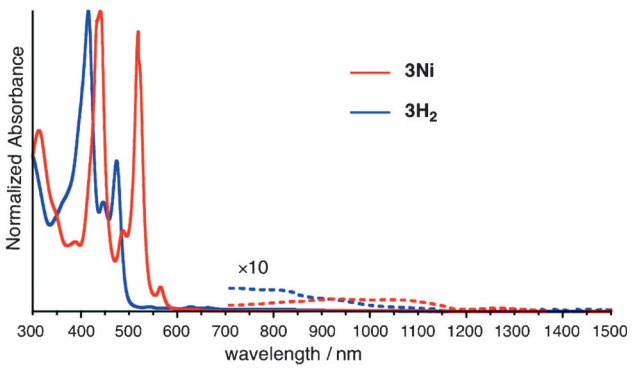

Figure 6. UV/Vis absorption spectra of **3Ni** and **3H$_2$** in CH_2Cl_2.

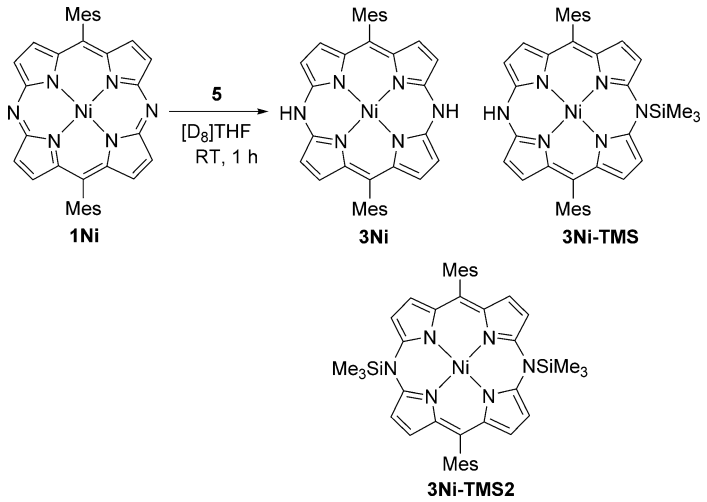

Scheme 6. Reaction of **1 Ni** with **5** in [D_8]THF.

3 H_2 showed reversible first oxidation waves at −0.717 and −0.534 V, respectively, suggesting the donating nature of **3 Ni** and **3 H_2**.

In summary, we have demonstrated the reagent-controlled chemo- and regioselective reduction of 5,15-diazaporphyrins **1 M**. The reduction of **1 M** with $NaBH_4$ provides the isobacteriochlorin-type product **2 M**, whereas antiaromatic dihydrodiazaporphyrins **3 M** was obtained through the reduction with *N*,*N*′-bis(trimethylsilyl)-1,4-dihydropyrazine **5**. This is the first example of antiaromatic porphyrinoids bearing a conjugation circuit including the lone pairs on the nitrogen atoms at the *meso* positions.[20,21] The methodology described herein provides a new route for the creation of antiaromatic compounds and will open up the chemistry of antiaromatic heteroporphyrinoids. Further investigation of the unique properties of **3 M** is currently in progress in our group.

Acknowledgements

We thank Kento Kawakita and Haruka Nishiyama (Osaka University) for their help with the preparation of **5**. This work was supported by Grant-in-Aids for Scientific Research on Innovative Areas, "π-System Figuration" (26102003) and "Element Blocks" (25102514) and the Program for Leading Graduate Schools "Integrative Graduate Education and Research in Green Natural Sciences", MEXT, Japan. H.S. acknowledges the Asahi Glass Foundation for financial support.

Keywords: antiaromaticity · chemoselectivity · porphyrinoids · reduction · tautomerism

[1] a) *Handbook of Porphyrin Science, Vol. 17* (Eds.: K. M. Kadish, K. M. Smith, R. Guilard) World Scientific, Singapore, **2012**; b) H. W. Whitlock Jr., R. Hanauer, M. Y. Oester, B. K. Bower, *J. Am. Chem. Soc.* **1969**, *91*, 7485; c) W. B. T. Cruse, P. J. Harrison, O. Kennard, *J. Am. Chem. Soc.* **1982**, *104*, 2376; d) F.-P. Montforts, B. Gerlach, F. Hoeper, *Chem. Rev.* **1994**, *94*, 327; e) A. Ghosh, *Acc. Chem. Res.* **1998**, *31*, 189.

[2] B. Krattinger, H. J. Callot, *Eur. J. Org. Chem.* **1999**, 1857.

[3] a) R. B. Woodward, *Angew. Chem.* **1960**, *72*, 651; b) M. Pohl, H. Schmickler, J. Lex, E. Vogel, *Angew. Chem. Int. Ed. Engl.* **1991**, *30*, 1693; *Angew. Chem.* **1991**, *103*, 1737.

[4] C. Liu, D.-M. Shen, Q.-Y. Chen, *J. Am. Chem. Soc.* **2007**, *129*, 5814.

[5] a) J. A. Cissell, T. P. Vaid, A. L. Rheingold, *J. Am. Chem. Soc.* **2005**, *127*, 12212; b) H. Song, J. A. Cissell, T. P. Vaid, D. Holten, *J. Phys. Chem. B* **2007**, *111*, 2138.

[6] a) J. Setsune, K. Kashihara, K. Wada, H. Shiozaki, *Chem. Lett.* **1999**, 847; b) A. Weiss, M. C. Hodgson, P. D. W. Boyd, W. Siebert, P. J. Brothers, *Chem. Eur. J.* **2007**, *13*, 5982; c) T. P. Vaid, *J. Am. Chem. Soc.* **2011**, *133*, 15838.

[7] For antiaromatic 20π core-modified porphyrinoids, see: a) J. S. Reddy, V. G. Anand, *J. Am. Chem. Soc.* **2008**, *130*, 3718; b) E. Vogel, W. Haas, B. Knipp, J. Lex, H. Schmickler, *Angew. Chem. Int. Ed. Engl.* **1988**, *27*, 406; *Angew. Chem.* **1988**, *100*, 445; c) T. Nakabuchi, M. Nakashima, S. Fujishige, H. Nakano, Y. Matano, H. Imahori, *J. Org. Chem.* **2010**, *75*, 375.

[8] For β-unsubstituted diazaporphyrins, see: a) M. Horie, Y. Hayashi, S. Yamaguchi, H. Shinokubo, *Chem. Eur. J.* **2012**, *18*, 5919; b) A. Yamaji, S. Hiroto, J.-Y. Shin, H. Shinokubo, *Chem. Commun.* **2013**, *49*, 5064; c) A. Yamaji, J.-Y. Shin, Y. Miyake, H. Shinokubo, *Angew. Chem. Int. Ed.* **2014**, *53*, 13924; *Angew. Chem.* **2014**, *126*, 14144; d) Y. Matano, T. Shibano, H. Nakano, H. Imahori, *Chem. Eur. J.* **2012**, *18*, 6208; e) Y. Matano, T. Shibano, H. Nakano, Y. Kimura, H. Imahori, *Inorg. Chem.* **2012**, *51*, 12879; f) S. Omomo, Y. Maruyama, K. Furukawa, T. Furuyama, H. Nakano, N. Kobayashi, Y. Matano, *Chem. Eur. J.* **2015**, *21*, 2003; g) F. Abou-Chahine, D. Fujii, H. Imahori, H. Nakano, N. V. Tkachenko, Y. Matano, H. Lemmetyinen, *J. Phys. Chem. B* **2015**, *119*, 7328; h) S. Omomo, K. Furukawa, H. Nakano, Y. Matano, *J. Porphyrins Phthalocyanines* **2015**, *19*, 775; i) Y. Matano, D. Fujii, T. Shibano, K. Furukawa, T. Higashino, H. Nakano, H. Imahori, *Chem. Eur. J.* **2014**, *20*, 3342; j) M. Yamamoto, Y. Takano, Y. Matano, K. Stranius, N. V. Tkachenko, H. Lemmetyinen, H. Imahori, *J. Phys. Chem. C* **2014**, *118*, 1808.

[9] For β-substituted diazaporphyrins, see: a) H. Fischer, H. Haberland, A. Müller, *Justus Liebigs Ann. Chem.* **1936**, *521*, 122; b) H. Ogata, T. Fukuda, K. Nakai, Y. Fujimura, S. Neya, P. A. Stuzhin, N. Kobayashi, *Eur. J. Inorg. Chem.* **2004**, 1621; d) H. Shinmori, F. Kodaira, S. Matsugo, S. Kawabata, A. Osuka, *Chem. Lett.* **2005**, *34*, 322; e) P. A. Stuzhin, O. G. Khelevina, *Coord. Chem. Rev.* **1996**, *147*, 41; f) Y. Ohgo, S. Neya, H. Uekusa, M. Nakamura, *Chem. Commun.* **2006**, 4590; g) P. A. Stuzhin, S. E. Nefedov, R. S. Kumeev, A. Ul-Haq, V. V. Minin, S. S. Ivanova, *Inorg. Chem.* **2010**, *49*, 4802; h) P. A. Stuzhin, A. Ul-Haq, S. E. Nefedov, R. S. Kumeev, O. I. Koifman, *Eur. J. Inorg. Chem.* **2011**, 2567; i) T. Okujima, G. Jin, S. Otsubo, S. Aramaki, N. Ono, H. Yamada, H. Uno, *J. Porphyrins Phthalocyanines* **2011**, *15*, 697; j) N. Pan, Y. Bian, T. Fukuda, M. Yokoyama, R. Li, S. Neya, J. Jiang, N. Kobayashi, *Inorg. Chem.* **2004**, *43*, 8242; k) N. Pan, Y. Bian, M. Yokoyama, R. Li, T. Fukuda, S. Neya, J. Jiang, N. Kobayashi, *Eur. J. Inorg. Chem.* **2008**, 5519; l) R. L. N. Harris, A. W. Johnson, I. T. Kay, *J. Chem. Soc. C* **1966**, 22.

[10] a) S. Eu, S. Hayashi, T. Umeyama, Y. Matano, Y. Araki, H. Imahori, *J. Phys. Chem. C* **2008**, *112*, 4396; b) C. Matlachowski, M. Schwalbe, *Dalton Trans.* **2013**, *42*, 3490.

[11] CCDC 1440694 (**2 Ni**) contains the supplementary crystallographic data for this paper. These data can be obtained free of charge from The Cambridge Crystallographic Data Centre. Crystallographic data for **2 Ni**: $C_{36}H_{34}Cl_6N_6Ni$; $M_w = 609.40$; monoclinic; $P2_1/c$; $a = 8.0857(11)$, $b = 25.718(3)$, $c = 7.1564(10)$ Å; $\beta = 108.2820(10)^\circ$; $V = 1413.1(3)$ Å^3; $Z = 2$; $R = 0.0371$ ($I > 2.0\ \sigma(I)$); $R_w = 0.1001$ (all data); GOF = 1.105.

[12] a) W. Kaim, *J. Am. Chem. Soc.* **1983**, *105*, 707; b) T. Saito, H. Nishiyama, H. Tanahashi, K. Kawakita, H. Tsurugi, K. Mashima, *J. Am. Chem. Soc.* **2014**, *136*, 5161; c) T. Yurino, Y. Ueda, Y. Shimizu, S. Tanaka, H. Nishiyama, H. Tsurugi, K. Sato, K. Mashima, *Angew. Chem. Int. Ed.* **2015**, *54*, 14437; *Angew. Chem.* **2015**, *127*, 14645.

[13] CCDC 1440696 (**3 Ni**) contains the supplementary crystallographic data for this paper. These data can be obtained free of charge from The Cambridge Crystallographic Data Centre. Crystallographic data for **3 Ni**: $C_{36}H_{32}N_6Ni$; $M_w = 607.38$; monoclinic; $P2_1/c$; $a = 13.167(4)$, $b = 13.763(4)$,

$c = 8.129(3)$ Å; $\beta = 103.122(4)^\circ$; $V = 1434.6(8)$ Å^3; $Z = 2$; $R = 0.0383$ ($I > 2.0\,\sigma(I)$); $R_w = 0.0899$ (all data); GOF = 1.090.

[14] CCDC 1440695 (**3H$_2$**) contains the supplementary crystallographic data for this paper. These data can be obtained free of charge from The Cambridge Crystallographic Data Centre. Crystallographic data for **3H$_2$**: $C_{40}H_{40}N_8$; $M_w = 632.80$; monoclinic; space group $P2_1/n$; $a = 7.5045(19)$, $b = 9.607(2)$, $c = 24.478(6)$ Å; $\beta = 97.097(5)^\circ$; $V = 1751.2(8)$ Å^3; $Z = 2$; $R = 0.0474$ ($I > 2.0\,\sigma(I)$); $R_w = 0.1310$ (all data); GOF = 1.071.

[15] For hydrogen bonding interactions in antiaromatic porphyrinoids, see: a) S. Shimizu, W. Cho, J. L. Sessler, H. Shinokubo, A. Osuka, *Chem. Eur. J.* **2008**, *14*, 2668; b) H. Mori, Y. M. Sung, B. S. Lee, D. Kim, A. Osuka, *Angew. Chem. Int. Ed.* **2012**, *51*, 12459; *Angew. Chem.* **2012**, *124*, 12627; c) K. Naoda, H. Mori, J. Oh, K. H. Park, D. Kim, A. Osuka, *J. Org. Chem.* **2015**, *80*, 11726.

[16] a) C. B. Storm, Y. Reklu, *J. Am. Chem. Soc.* **1972**, *94*, 1745; b) R. J. Abraham, G. E. Hawkes, K. M. Smith, *Tetrahedron Lett.* **1974**, *15*, 1483; c) S. S. Eaton, G. R. Eaton, *J. Am. Chem. Soc.* **1977**, *99*, 1601; d) J. Braun, M. Schlabach, B. Wehrle, M. Köcher, E. Vogel, H.-H. Limbach, *J. Am. Chem. Soc.* **1994**, *116*, 6593.

[17] J. Sandström, *Dynamic NMR Spectroscopy*, Academic Press, London, **1982**, p. 96.

[18] F.-G. Klärner, *Angew. Chem. Int. Ed.* **2001**, *40*, 3977; *Angew. Chem.* **2001**, *113*, 4099.

[19] a) S. Mori, A. Osuka, *J. Am. Chem. Soc.* **2005**, *127*, 8030; b) T. Ito, Y. Hayashi, S. Shimizu, J.-Y. Shin, N. Kobayashi, H. Shinokubo, *Angew. Chem. Int. Ed.* **2012**, *51*, 8542; *Angew. Chem.* **2012**, *124*, 8670.

[20] Very recently, Kobayashi and co-workers have reported antiaromatic azaporphyrinoids based on superphtalocyanines having imine sp^2-hybridized nitrogen atoms in the conjugation circuit, see: T. Furuyama, T. Sato, N. Kobayashi, *J. Am. Chem. Soc.* **2015**, *137*, 13788.

[21] After submission of our manuscript, Matano and co-workers have independently reported the synthesis of 20π antiaromatic *N*,*N*′-diaryldiazaporphyrin Ni^{II} complexes. T. Satoh, M. Minoura, H. Nakano, K. Furukawa, Y. Matano, *Angew. Chem. Int. Ed.* **2016**, *55*, DOI: 10.1002/anie.201510734; *Angew. Chem.* **2016**, *128*, DOI: 10.1002/ange.201510734.

Received: January 7, 2016
Published online on February 3, 2016